DROP-WEIGHT IMPACT LOADING TESTS OF THROUGH-TYPE STEEL-POST MODELS FOR ROCKFALL PROTECTION FENCE

Satoshi Kondo[1], Masato Komuro[2], Norimitsu Kishi[3], Yasuhiro Yamamoto[4]

In order to establish a rational design procedure for the steel posts of the rockfall-protection fence built into the concrete retaining walls, static and drop-weight impact loading tests were conducted on through-type H-section steel-post models installed in the plain-concrete foundation varying the length of the moment arm. The results obtained from this study were as follows: 1) a plastic hinge was formed in the post model near the base of the footing under static and impact loading regardless of the length of the moment arm and 2) the anchoring depth specified in the current design guideline tends to be safety side in design based on the comparison with the experimental results under impact loading.

Keywords: rockfall protection fence, steel post, impact loading, anchoring depth

INTRODUCTION

In Japan, road networks have been constructed along cliffs and slopes in the mountain areas. On the cliff side of roads, rockfall protection fences are embedded in the top-surface region of the retaining wall to ensure the safety of human lives and transportation networks from falling rocks as shown in Fig. 1 [1]. Generally, the rockfall retaining walls were designed as gravity type plain-concrete structures. Therefore, the steel posts of the fences were embedded into the box-shaped excavated holes at the top-surface of the walls.

Today, these steel posts are designed following the design guideline for rockfall countermeasures [2] (hereinafter, guideline) in Japan. However, the dynamic response characteristics of the posts and the wall due to rockfall impact were not taken into account in the guideline, the impact loads being assumed as static loads. Therefore, in order to ensure safety of the passengers and transportation networks from falling rocks, it is an urgent matter to establish an appropriate design procedure for the steel posts of rockfall protection fences taking the impact-resistant characteristics into account.

From this point of view, in this study, to investigate the dynamic response characteristics of the posts and the concrete wall, the static and impact loading tests for the steel post models, which are supported by embedding in the plain-concrete block, were conducted.

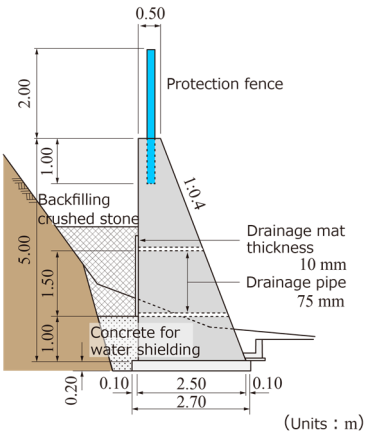

Fig. 1 Rockfall protection retaining wall with embedded steel post for fence

EXPERIMENTAL OVERVIEW

Figure 2 shows the dimensions of the test specimens and rebar arrangement. The concrete block

[1] Sunago Co., Ltd., Naie, Hokkaido 079-0394, Japan, s.kondo@sunagonet.co.jp
[2] Muroran Institute of Technology, Muroran 050-8585, Japan, komuro@mmm.muroran-it.ac.jp
[3] Muroran Institute of Technology, Muroran 050-8585, Japan, kishi@mmm.muroran-it.ac.jp
[4] Sunago Co., Ltd., Naie, Hokkaido 079-0394, Japan, y.yamamoto@sunagonet.co.jp

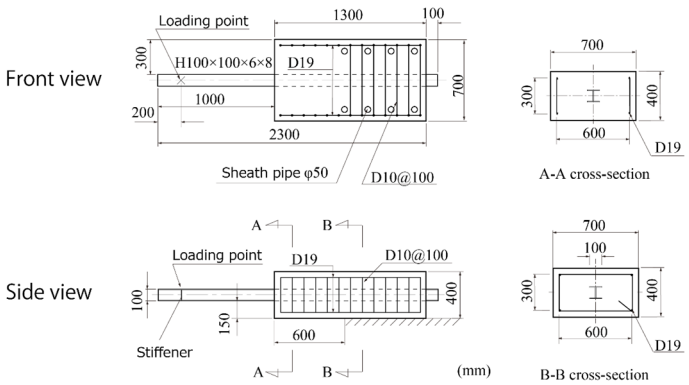

Fig. 1 Dimensions of test specimen and rebar arrangement for Post B

(a) Static loading (b) Impact loading

Fig.2 View of experimental set-up

specimens, as the foundation and anchorage, have the dimensions 700 × 400 × 1,300 mm (width × height × length), in which a part of the length of 600 mm measured from its front-surface (hereinafter, base) was taken as the footing for the post model and the other part as the anchorage of the model. In order to minimize the reinforcing effects of the rebars on the load-carrying capacities of the footing, the axial rebars and stirrups were placed near the side-surfaces of the footing as shown in the A-A cross-section of Fig. 1.

H-section steel members of 100 mm width and height were used for the post model. The loading points for the model were taken, respectively, at the locations of 800 mm (designated as Post B) and 400 mm (designated as Post S) from the base of the footing for bending action and bending-shear action to be predominant. The 6 mm thick stiffener plates were welded to the flanges and the web of the models at the loading point to restrain local buckling. The foundations were anchored to the rigid steel frames by fastening with bolts and nuts.

The drop-weight impact loading tests were conducted following a single loading method, in which a steel weight with a mass of 300 kg and a tip diameter of 200 mm was allowed to drop freely onto the post model from the prescribed height once only. The static loading tests were also conducted by using a hydraulic jack. Figure 2 shows the test set-ups for static and impact loading.

The measuring items were impact force, axial strain distributions of the web for the post models, and vertical displacements of the specimens. Strain gauges were glued at 30 mm upper and lower points from the mid-height of the web of the models.

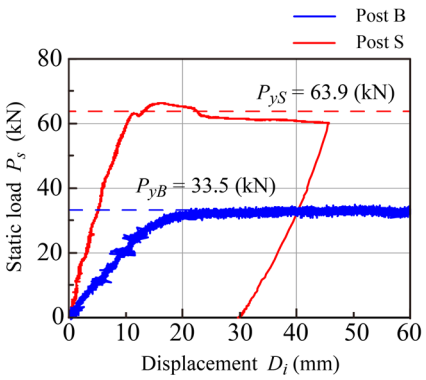

Fig. 3 Comparison of load-displacement curves under static loading

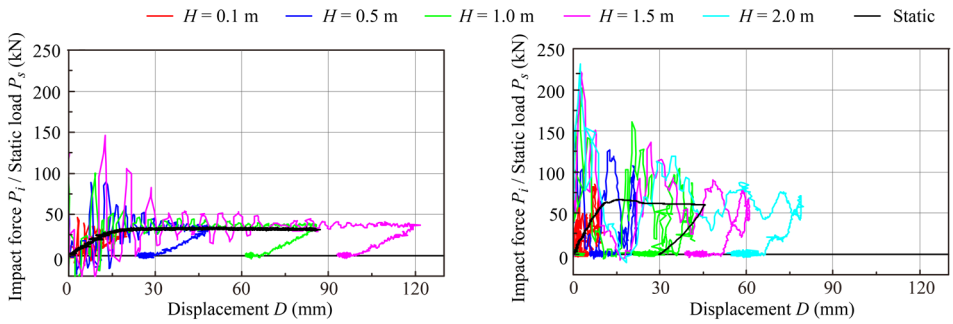

(a) Post B (b) Post S

Fig. 4 Comparisons of hysteresis loops between impact forces P_i/static load P_s and displacement D

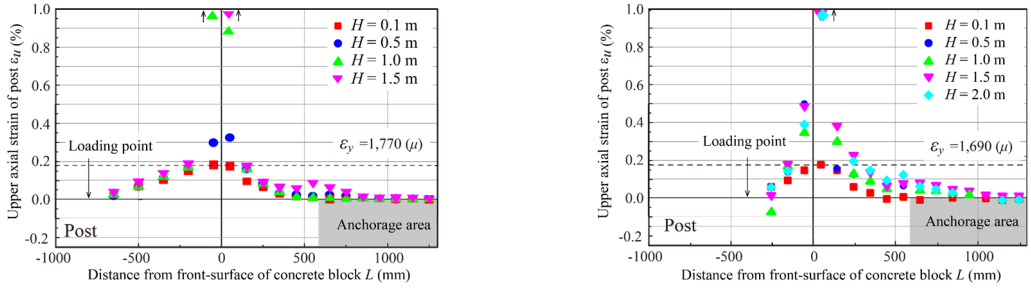

(a) Post B (b) Post S

Fig. 5 Comparisons of upper fiber strain distributions for post at maximum response

EXPERIMENTAL RESULTS AND DISCUSSION

Figure 3 shows comparisons of the load P_s-displacement D at the loading point (hereinafter, displacement) curves obtained from the static loading tests. In this figure, the calculated yield loads P_y of the post models are shown, which were estimated assuming the base of the footing as the fixed point and using the calculated yield moment and section modulus. From this figure, it is observed that both yield loads P_{yB} and P_{yS} were approximately same to the maximum load for each specimen. This means that both post models might not be perfectly fixed at the base of the footings. Since both curves are flattened, the plastic hinges may have been formed in the posts near the base of the footing.

Figure 4 shows the hysteresis loops between impact force P_i/static load P_s and displacement D for posts B and S. From this figure, it is observed that: (1) in the case of Post B, even though the alternative load components of high amplitude were predominant up to a displacement D = 30 mm, the loops approached closely the force forming the plastic hinge statically; (2) in the case of Post S, the amplitude of the alternative loads was larger than those of Post B; however, (3) the average value of the force was similar to that for the static load-displacement relationship.

Figure 5 shows comparisons of the upper axial strain distributions for the posts at the maximum response for varying drop height of the weight. From these figures, the following details can be observed: (1) at drop height H = 0.1 m the strains were linearly and elastically distributed from the loading point and the strains decreased to approximately zero at 500 mm distance from the base of the footing in both Posts B and S; (2) at H = 1 m, since the strains significantly exceeded the yield strain near the base of the footing for both posts, a plastic hinge might be formed

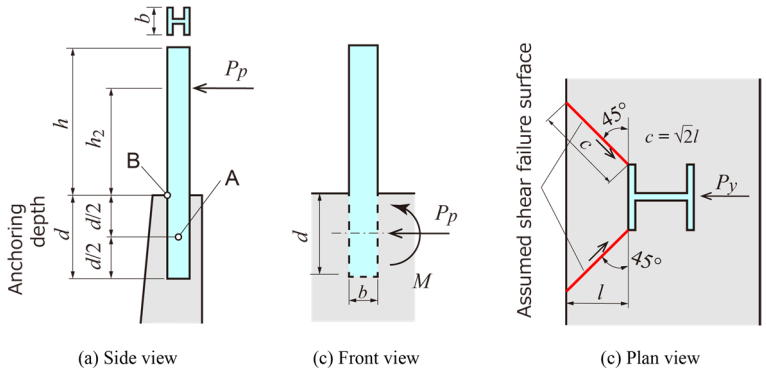

Fig. 6 Schematic diagram for designing anchoring depth of fence

around those areas; and (3) the strains in the footing tended to zero at around L = 500 mm from the base in the case of Post B; however, (4) anchoring depth cannot be appropriately evaluated due to a negative bending at the fixing boundary of footing prevailing.

ANCHORING DEPTH OF POST

In the guideline [2], the anchoring depth of the posts in the footing is specified as to be determined by checking the bearing stress for a short pillar model with depth d as the anchoring depth and shear stress acting on the assumed shear failure surface developed in the direction of 45º from the edges of the flange of the post as shown in Fig. 6. An applied load P_p is determined by forming a plastic hinge at the base of the footing and the equivalent axial force P_p and bending moment M are modeled to act at the center of the short pillar model as shown in Fig. 6(b). The calculated bearing stress and shear stress must be less than these allowable stresses.

The required anchoring depth d of the post following the current specification [2] described above was evaluated as 671 mm, for both of Posts B and S. Determining the anchoring depth obtained from the experimental results at drop height H = 0.1 m as L = 500 mm as mentioned above, this may be smaller than those according to the specification [2].

CONCLUSIONS

In this paper, in order to investigate the dynamic behavior and actual anchoring depth of the posts for the fences installed in rockfall protection retaining walls, static and impact loading tests were carried out for the specimens. The specimens consisted of a through-type H-section steel post embedded in the foundation model. The results obtained from this study can be summarized as follows:

1. The H-section steel post models reached the ultimate state forming a plastic hinge near the base of the footing under both static and impact loading; and
2. The anchoring depth of the post in the footing obtained from the experimental results under impact loading may be smaller than the specific design value.

REFERENCES

[1] Japan River Association, “Technical criteria for river works of Ministry of Construction (Draft), Commentary, Part II Design.” 2017. [In Japanese]

[2] Japan Road Association, “Design guideline for rockfall countermeasures.” 2017. [In Japanese]